Effects of a Switched Weak Magnetic Field on Lecithin Liposomes, Investigated by Nonlinear Dielectric Spectroscopy

Alexander Pazur

Department Biologie 1 Universität München – Bereich Botanik, Menzingerstr. 67, D-80638 München. Fax: 089-17861-185. E-Mail: pazur@botanik.biologie.uni-muenchen.de

Z. Naturforsch. **58c**, 386–394 (2003); received December 5, 2002/January 10, 2003

Three types of liposomes in aqueous solution were subjected to a low frequency switched weak magnetic field. A differential non-linear dielectric spectroscopy (DNLDS) was performed at 40 °C with two planar orthogonal electrodes, positioned parallel and vertical to the earth surface. The difference of the free voltage release (FVR) signals for the two orthogonal directions following electric pulses with an amplitude of 1.0 V and a duration of 25 ms, were *Fourier*-transformed. An additional magnetic field was switched with a period of 400 ms and a variable amplitude from 0 to 100 G, whose direction was parallel to the vertical electrode plane. With two of the liposomes (egg yolk lecithin (EY), asolectin doped with cholesterol (ASCO)) a decrease of the signal amplitude with increasing magnetic fields could be seen in most of the 25 observed harmonic frequencies (relative to the electric pulse frequency f(0) = 40 Hz). For EY liposomes this decrease was highly significant and not linear for the 1.–5., and above the 20. harmonic frequency, ASCO liposomes showed a similar effect. Asolectin liposomes showed the reverse response.
Quantum mechanical conditions of charges on the liposome surface are discussed as a possible origin of these effects.

Key words: Liposome, Biological Magnetic Field Effect, Nonlinear Dielectric Spectroscopy (NLDS)

Introduction

The investigation of biological effects caused by magnetic fields and non-ionizing electromagnetic radiation probably began in the late 19th century in Russia (mentioned by Zhadin, 2001). While in the early studies natural sources like the earth's magnetic field were in the focus of interest, more recent ones were aimed to recognize potential human health risks by man-made environmental factors (WHO, 1984; WHO, 1987). On the other hand, a potential was predicted and partially found for medical diagnostic and therapy by the use of specific magnetic fields and low frequency electromagnetic radiation. Examples were reported for orthopedics (Darendeliler *et al.*, 1997), neurology (Crasson *et al.*, 1999), and cancer research (Chakkalakal *et al.*, 1999).

Three physical mechanisms have been discussed, underlying biological effects of weak (< 1000 G) magnetic fields: the presence of ferromagnetic particles, chemical reactions modulated by singlet-triplet mixing of radical pairs, and the ion cyclotron resonance (ICR). Ferromagnetic mechanisms where mainly investigated in microorganisms (Torres de Araujo *et al.*, 1986), they are understood by mechanical action of the particles on the host cell. They have also been invoked for the "compass mechanism" *e.g.* of migration birds (Deutschlander *et al.*, 1999; Wiltschko *et al.*, 2000). The fundamentals of the "radical pair mechanism", involving the modulation of singlet-triplet interconversion rates by weak fields, were studied on photosynthetic reaction centers and the respiratory chain (Rademaker *et al.*, 1980; Ogrodnik *et al.*, 1982; Waliszewski *et al.*, 1999). This effect has also been proposed as the origin of magnetic orientation in several animals, where the receptors are linked to the visual system. Magnetically induced cyclotron resonances of ions in aqueous solutions, which can shift the equilibrium of biochemical reactions in presence of weak static magnetic fields, are suggested by Liboff (1997) and

Abbreviations: AS, soybean lecithin (asolectin); ASCO, asolectin-cholesterol mixture; DNLDS, differential non linear dielectric spectroscopy; ELF, extremely low frequency; EY, egg yolk lecithin; FVR, free voltage release; ICR, ion cyclotron resonance; NLDS, non linear dielectric spectroscopy.

0939–5075/2003/0500–0386 $ 06.00

Adair (1997), who estimate field strengths of some Gauss and correlating frequencies for this mechanism. Smith *et al.* (1995) investigated ICRs for Ca^{2+}, K^+ and Mg^{2+} by germination experiments with radishes in suitable alternating weak magnetic fields. Zhadin *et al.* (1998) found an increasing ionic current at the ICR condition of a glutamic acid solution, applying combined static and alternating magnetic fields at intensities of some μT.

There is increasing evidence for the involvement of membranes, in combination with one or several of the above mentioned mechanisms. A mechanism was proposed by Yee *et al.* (1994), in which, nearby the trasition temperature T_c, different phase states of a lipid mixture can coexist, caused by large concentration gradients. Ramundo-Orlando *et al.* (2000a, b) investigated the involvement of charged lipids and carbonic anhydrase, a peripheral enzyme, in dipalmitoyl-phosphatidlycholine liposomes exposed to ELF fields. At 7 Hz, an increased permeability was observed, for liposomes containing stearylamine. An increased permeability of cell membranes of barley seeds is reported by Khizhenkov *et al.* (2001) during soaking with Pb^{2+}, Ba^{2+}, Na^+, K^+ under the action of ELF fields in the range < 1 G. In summary, these data indicate that membranes are involved in biological magnetic field effects, probably relating to singlet-triplet mixing, or ICR mechanisms.

In the present work results are reported, which show changes of dielectric properties of liposomes with different lipid compositions above the transition temperature, when a low frequently switched magnetic field of relative low intensity (≤ 100 G) is applied.

Materials and Methods

Liposome preparation

Three types of liposomes were prepared: (a) from egg yolk lecithin (EY, Merck 1.05331.0100), (b) soybean lecithin (AS asolectin, Fluka 11145), and (c) an asolectin cholesterol (10% w/w) mixture (ASCO, cholesterol from Sigma C8667). The lecithins were prepurified by washing them twice with acetone, drying in a vacuum desiccator, and storage under argon for further use. Molecular properties, chain lengths, and a mean mol weight of 734.1 were assumed as in Bultmann *et al.* (1991). The suitable buffer used in all experiments was that of Matsuzaki (2000), containing NaCl (150 mM), Tris-hydroxymethyl-aminomethane (10 mM), EDTA (1 mM) adjusted with HCl to pH 7.0. It was degassed and stored under an argon atmosphere, to reduce lipid oxidation. The lipids were dissolved in chloroform and transfered into test tubes for sonication, yielding a final concentration of 0.5% w/w lecithins. After quick evaporation of the solvent by flushing with argon, 40 ml buffer were added, and the mixture shaken by hand for 30 s in order to mix the components without using solvents or detergents, as described by Christopher *et al.* (1984), and Collins (1995). The emulsion was sonified for 20 min. (Branson Sonifier W-450, 50% power, 50% duty cycle, at 20° C), comparable with the treatment suggested by Levchuk *et al.* (1983) for preparing unilamellar liposomes. The obtained stock probes were centrifuged ($2000 \times g$, at 4° C) for 2 min to remove titanium abrasions from the tip caused by the ultrasonication. The supernatants were stored at + 4° C in the dark under argon, and could be used for up to one week. Mean liposome sizes were estimated by the right angle light scattering method of Matsuzaki *et al.* (2000) using a spectrofluorimeter (Spex Fluorolog 1680, Spex Industries, Munich).

Measurement principle

The NLDS technique was developed during the past decade with the aim of obtaining size-, shape- and surface-information for cells and smaller particles in aqueous solutions, by using a relatively simple electrochemical measuring apparatus. In the simplest case, a sinusoidal alternating electric field is applied to the solution by 2 electrodes, using peak to peak voltages of 0.5–1.5 V and frequencies of 1 to 1000 Hz. Particles with a relative dielectric constant different from that of their environment (pure water: $\varepsilon_r = 80.8$) distort the field, thereby inducing alternating voltages over and currents through the solution, which are detected by 2 auxiliary electrodes in order to avoid polarisation effects. The distortions of the obtained signals contain the underlying spectral information. Therefore the signals are *Fourier*-transformed and evaluated as spectra in the frequency domain (see McShea *et al.*, 1992, Woodward *et al.*, 1996; 2000).

The general behavior of particles in an electric field $\boldsymbol{E}$, is illustrated in Fig. 1, where measurement

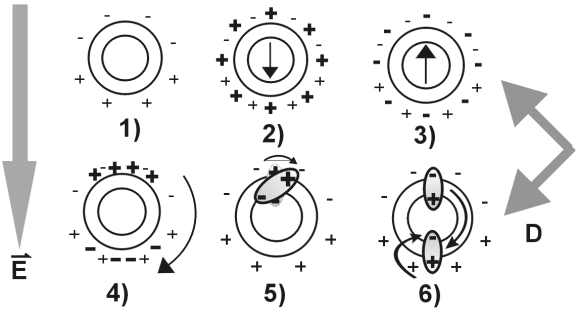

Fig. 1. The behavior of liposomes (and other particles with a dielectric surface) in an electric field ***E***, and orientation of the perpendicular electrodes **D**, each at 45 ° against the direction of the electric field ***E***:
1) Liposomes of uncharged lipids: Polarizing effect of ***E*** induces dipoles with opposite orientation as ***E*** (shown in all 6 examples by thin + and – signs). This induced dipoles distort the external potential with a specimen-characteristic time constant. The resulting NLDS signals of electrodes in the two perpendicular planes **D** have equal amplitudes with opposite (180°) phases, which cancel upon subtraction.
2–3) Liposomes with a uniform positive (2) or negative (3) surface charge (bold symbols) additionaly move in the electric field up or down, on account of their net-charges. These signals vanish too upon subtraction, because their phases are also shifted by 180°. All other charge distributions generate dipole-moments, which cause direction dependent potential changes and yield a non-zero difference signal for the two monitoring directions **D**.
4) Fixed but unequal distributed surface charges effect rotation of the particle.
5–6) A fluid lipid matrix allows moving and turning around of charged molecules in the membrane plane.

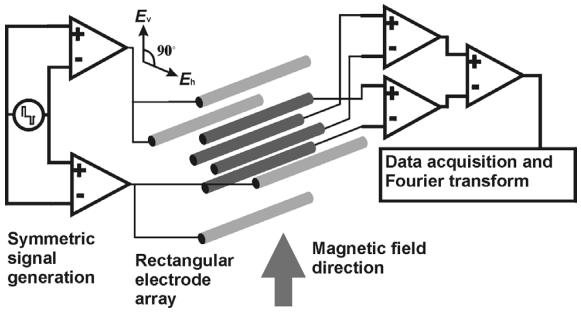

Fig. 2. The DNLDS electrode array consists of two electrode planes rectangular to each other (thin arrows). Every plane consists of 4 parallel arranged identical platinum wires. The outer wires (light grey) of this cross-formed arrangement are pairwise connected to the symmetric output of the signal generator, which drives the vertical and horizontal directed electric fields (E_v, E_h). The inner electrode wires (dark grey) are pairwise connected to the two symmetric input channels of the pre-amplifier, which allows formation of the difference signal for further data acquisition. When a magnetic field was applied, its direction was perpendicular to the electrodes (fat arrow).

is done with 2 pairs of electrodes (***D***) inclined by ± 45° against the direction of the electric field ***E***.

Apparatus

In the present work, the "standard" NLDS experimental setup was modified: Fig. 2 shows schematically the DNLDS (differential non linear dielectric spectroscopy) setup with planes at right angle, each with 4 single platinum electrodes. Several reports focus on finding proper electrode materials and their pre-treatment for good electric long-term stability (Woodward *et al.*, 1996; Yardley *et al.*, 2000). Cleaning with chloroform is followed by ultrasonication in a detergent solution (0.5% Triton X-100), washings with $CaCl_2$ (0.5 M in water) and finally deionized water (< 2 μS) resulted in acceptable signal stability (deviation of correponding amplitudes ≤ 5%) over an experimental session of up to 2 h. Always two adjacent outer electrodes were connected with one of the 2 outputs of a differential signal driver. Small mechanical differences of the two electrode planes were electrically compensated in order to obtain equal electric field strengths for both directions. This arrangement leads to a more homogeneous ***E*** field then a simple application with 2 perpendicular electrodes, each at 45° to the inner signal detection electrodes. Furthermore it will allow the use of a rotating quadrupole field in future investigations. Each pair of the inner electrodes was connected to one of two differential preamplifiers, whose output signals could be balanced by a potentiometer. Acquisition, digitalization, *Fourier* transformation and storage of the data was performed by a Pentium computer equipped with a DA/AD-converter board (Lab-PC+, National Instruments, Austin TX U. S. A.). The magnetic field was applied perpendicular to the electrodes by a suitably controled solenoid (Pazur, 2001).

The probe volume of 5 ml with the electrodes immersed, was kept at a constant temperature of 40 ± 0.2 °C by a water thermostate, ensuring that lipid phases were safely above their transition temperatures (Bultmann *et al.*, 1991). This was ascertained by the results of DNLDS measurements at several temperatures: Reproducible changes of the

spectra were observed, when traversing the temperature ranges were the transition temperatures were expected. Electrode polarisation effects and sedimentation of the liposomes were minimized by a short pneumatic mixing (0.5 ml/1 s) of the probe by an electronically controlled pipettemechanism, before each individual measurements.

Applied signals

The signal timing diagrams are shown in Fig. 3 (A–D). The total recording time for one spectrum is 400 ms. (A) shows the magnetic signal, which is present during the whole 400 ms time window, changes its polarity after 200 ms, and whose intensity can be varied from 0–100 G. In order to excite a broad frequency range for the DNLDS, rectangular electrical pulses (1 V) were applied with changing polarity, lasting 25 ms each, beginning at every half-time of the measuring period (B). The acquisition time (C) begins directly after the end of the half pulses and lasts to the end of the respective half-time (25–200 and 225–400 ms). In this time the FVR (free voltage release) is sampled, caused by the recombination of the induced dipoles. In case of a liposome-free conducting aqueous solution (buffer), the difference signal from the two orthogonal electrode pairs could be adjusted to zero. Introduction of liposomes resulted in decay signals like the ones schematically indicated in (D). The magnetic field switching was obtained by reversing the polarity after 200 ms, in phase with the reversal of the electric pulses. A complete experiment consisted of 101 spectra, during which the amplitude of the switched magnetic field was increased for every successive spectrum by ± 1 G from 0 to ± 100 G (0–10 mT). The pulse integral **Φ** for one individual measurement of 400 ms duration at the maximum field strength of 100 G is

$$\mathbf{\Phi} = B \cdot t = 100\ G \cdot 0.4\ s = 40\ Gs. \quad (1)$$

Reference experiments were executed identically, but without applying the magnetic field.

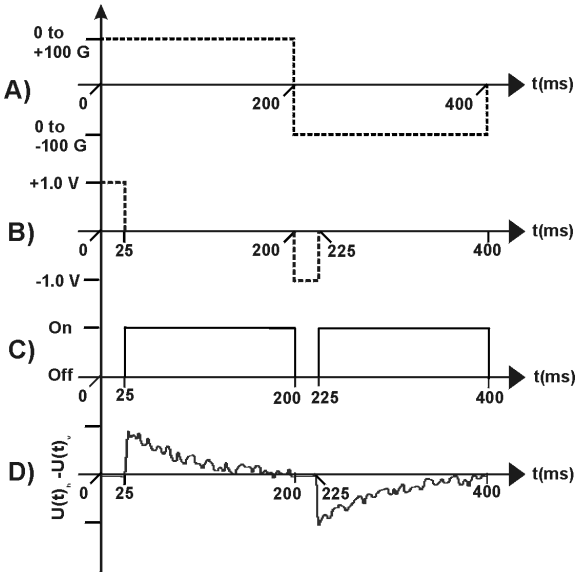

Fig. 3. Timing diagram of experiments:
A) Magnetic field: During a measuring cycle of 400 ms, the direction of the magnetic field was inverted after 200 ms. during a full measurement, the applied magnetic field was increased from 0 to 100 G in steps of 1 G.
B) Electric field: The driving electric pulses (1 V) for the outer electrode array lasted 25 ms at the beginning of each half periode, having opposite polarities in the two half-cycles.
C) Acquisition window: Sampling and recording of the FVR was started after switching off the electric pulses, viz. 25 ms after the beginning of each half period, and stopped at the end of the half period (indicated by the "on"- and "off"-position).
D) Example of the monitored difference signal (schematically). $U(t)_h$ is the horizontal, $U(t)_v$ the vertical monitored electrode voltage.

Results

The liposome solution could be introduced and withdrawn with a fixed syringe. This allowed for fast filling and rinsing of the unit, and replacement of the probes, without disassembling and need of new adjustment exactly to the center of the magnetic coil, for which the magnetic field strengths were appointed. Measurements were started after reaching the probe temperature of + 40 °C for at least 2 min by performing 10 spectral "dummy" scans without data acquisition to bring the electrodes to a stable dynamic equilibrium, then the actual experiment began. Every experiment was performed with a new probe. Control experiments with "used probes" showed an average activity loss with regard to magnetic field effects of 20% during the experiment.

Table I gives an overview of the experimental results, sorted by types of liposomes used. Each row belongs to one liposome or experiment type,

Table I. Summary of experimental data: The first two columns show kind and number of experiments.

	(2)	(3)	(4)	(5)	(6)
Liposome experiment type	No. of experiments	[1)] Mean liposome radius r (nm) at 40 °C	[2)]Transition temp. t_c (°C)	Voltage of first order DNLDS signal at start: U (mV)	linear regression of first order in% of start value: $y = r \cdot x$ + constant
EY (with magnetic field)	27	83.5 ± 1	29.5 ± 0.25	12.03 ± 0.54	− 0.32 · x + 86.9
EY (reference)	20			11.85 ± 0.49	+ 0.003 · x + 99.9
AS (with magnetic field)	16	76.0 ± 1	33.5 ± 0.25	7.11 ± 0.42	+ 0.15 · x + 100.7
AS (reference)	15			7.03 ± 0.40	− 0.010 · x + 101.4
ASCO (with magnetic field)	10	80.5 ± 1	31 ± 0.25	9.39 ± 0.50	− 0.16 · x + 97.5
ASCO (reference)	10			9.01 ± 0.64	− 0.008 · x + 101.2

[1)] Liposome radii were obtained by right angle light scattering.
[2)] t_c was obtained by DNLDS scans with stepwise increased temperatures (see "Materials and Methods").
The data in the column 5 shows the averaged signal voltages of the experiments for the first harmonic wave (order) at the beginning. The linear regressions of the normalized (start = 100%) growth of the first order signals are shown right. The experiments with applied magnetic field are grey shaded. The linear regression in column 6 ist expressed as usual by the gradient factor r and a constant, x is the magnetic field strength protracted on the abscissa (x-axis).

each column denotes one property. The total numbers of experiments were 27 (EY), 16 (AS), and 10 (ASCO) with a magnetic field, and 20 (EY), 15 (AS), and 10 (ASCO) without magnetic field (controls). Liposome radii and transition temperatures were investigated with 5 separate preparations each. By a 90° light scattering, EY liposomes show the largest size (r = 83.5 nm) at 40° C, AS liposomes are the smallest (r = 76.0 nm), and ASCO liposomes were intermediate (r = 80.5 nm).

The transition temperatures of the liposomes were studied using the DNLDS apparatus. The DNLDS spectra are generally smooth and reproducible over a large temperature range. However near the phase transition they show more or less chaotic signals in narrow temperature regions. These transition temperatures are shown in the Table I. A refinement of these methods will be the subject of further investigations.

The signals obtained by the FVR (see Fig. 3D) were *Fourier* transformed to yield the power (amplitude) spectra. Their abscissas were scaled in multiples of the base frequency $f(0)$ = 40 Hz ("orders" or "harmonic wave numbers" with respect to the electric pulse width of 25 ms, see Fig. 3B) for all further considerations. The absolute voltage amplitudes of the first order signals are shown for all liposome types in the 5th column of Table I. Under same conditions, all three liposome types show different DNLDS amplitudes. So it will be useful to normalize the data for comparison.

Fig. 4A shows the averaged spectra for 0 (dark line) and 100 G (grey dotted line) magnetic field intensity, averaged over all 27 experiments with EY liposomes. Up to the 7th order the signal is significantly reduced in the presence of the magnetic field. The ratio of the two spectra (Fig. 4B) further reveals, that their is a net decrease of only 25% in the middle frequency range (10. to 18. order) and a larger one for higher orders of $f(0)$, although the latter is not as pronounced as the one at the low frequency end of the spectrum. The residual signals were calculated after subtraction of the expected baselines. This baseline was obtained

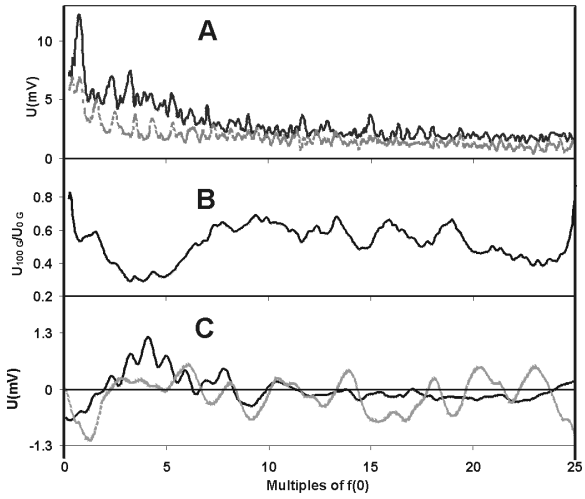

Fig. 4. A) The Fourier spectra from the DNLDS experiments with EY liposomes for 0 (black solid line) and 100 G magnetic field strength (grey dotted line). The X-scale is shown in multiples of $f(0)$, where $f(0)$ means the zero order frequency (40 Hz, resp. 25 ms) of the electric signal. The magnetic field impact causes a steeper decrease in some frequency ranges.
B) The distinction of the spectra for magnetic field strengths of **B** = 0 and 100 G, can be shown in detail by dividing the 100 G spectrum ($U_{100\,G}$) by the 0 Gs spectrum ($U_{0\,G}$). The ratio spectra are independent of the decreased intensities at increasing frequencies, due to the negative exponential (e^{-x}) decay of the amplitudes with rising frequency (x-axis). Local depressions are seen in the ranges about 4 and $23 \cdot f(0)$.
C) The residual signals after subtraction of the expected baselines (calculated by a curve fit for a e^{-x} function) of the spectra show the intensity deviation for discrete frequencies, compared with the spectrum of a pure squarewave signal (line styles like in diagram A): Lower intensities will be seen for frequencies $< 5 \cdot f(0)$ for the spectra at 100 G. At frequencies $> 15 \cdot f(0)$ the signal shows here also increased variations in several frequency ranges.

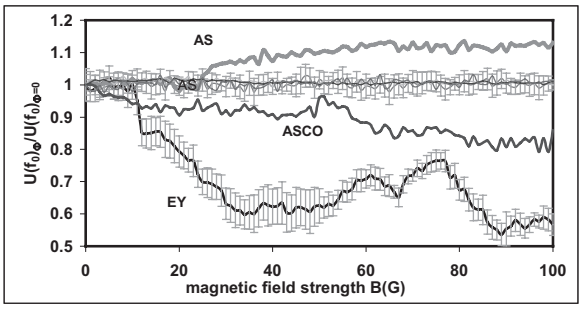

Fig. 5. Dependence of the first order (= $2 \cdot f(0)$) signal amplitudes on the intensity of the magnetic field strength for EY, AS, and ASCO liposomes. Data are averaged from all experiments. The signal ratios are calculated by dividing the data by the data for 0 G magnetic field strength.
Reference experiments were performed with the same timing and signal conditions, but with the magnetic field permanently switched off. The small fluctuations of the reference data indicate the noise of the used measuring system. Standard deviations are shown for EY and controls by vertical bars.

by a curve fit for a e^{-x} function. These data show the intensity deviation for discrete frequencies, compared with the spectrum of a pure squarewave signal (Fig. 4C).

Fig. 5 shows the intensity changes of the 1st orders of the DNLDS spectra with increasing magnetic field. The ordinate is normalized to the intensities at zero field. EY liposomes showed a strong decrease already at low magnetic field strengths, a slight increase between 50 and 75 G, and a final decrease to slightly more than 50% of the maximum intensity at zero field. AS liposomes showed a reverse field effect with a much smaller amplitude. The 1st order DNLDS signal rises monotonously by 15%. ASCO liposomes, which were doped with cholesterol, gave a decreasing signal, similar to the EY liposomes, but with a final less significant descent by only about 20%. The reference experiments without magnetic field showed no significant intensity changes. The relatively low standard deviations are indicated by the vertical bars for the experiments with EY liposomes. The right column of Table I shows additionally the linear regressions for the 1st order DNLDS signals, normalized to the corresponding value of the 1st spectrum of the experiments.

Discussion

The results provide evidence, that weak magnetic fields (< 100 G) and the magnetic components of ELF electromagnetic signals, have an effect on the electric properties of pure lipid membranes. Some recent studies have focused on natural membranes with frequency resolving measurement techniques like NLDS, whereby weak magnetic fields were applied before or during the measurements. Santini *et al.* (1995) reports a decrease of the electric conductivity and permittivity of K562 cells obtained by relaxation measurements considerably after exposure to ELF fields (50 Hz, 2.5 mT), whereas the conductivity of the

cytosol does not vary. Davies *et al.* (2000) found a strong nonlinear dielectric response of *Dictyostelium discoideum* cells after exposure to a pulsed magnetic field. We have previously reported a modified dielectric relaxation spectrum of undoped planar lipid membranes after exposure to weak magnetic pulses (Pazur, 2001). Here magnetic field effect was obviously caused by the pure lipid bilayer. In the following an estimation will be tried of membrane surface charge densities and their shifted energy levels by the magnetic field.

We make the following assumptions for our system:

- sphaerical, unilamelar liposomes with radius $\boldsymbol{r}_l = 8.35 \cdot 10^{-8}$ m
  (corresponding to EY liposomes, Table I)
- membrane thickness $d = 6$ nm

Right angle light scattering bases on total reflexion of the light, when passing from the optical denser to thinner medium at small incident angles. The liposome radii determined by this method should therefore represent those of the hydrophobic region of the membrane, with the largest refractive index difference at $d/2$. The liposome volume V_l, the "wall" volume V_w, and the outer surface $^A{}_l$ are given by:

$$V_l = \frac{4}{3} \cdot \pi \cdot \left(r_l + \frac{d}{2} \right)^3 \tag{2}$$

$$V_w = \frac{4}{3} \cdot \pi \cdot \left(\left(r_l + \frac{d}{2} \right)^3 - \left(r_l - \frac{d}{2} \right)^3 \right) \tag{3}$$

$$A_l = 4 \cdot \pi \cdot \left(r_l + \frac{d}{2} \right)^2 \tag{4}$$

The resulting values for EY liposomes are summarized in Table II, together with the derived values for the number of liposomes per ml, their average center-to-center distances, and their partial volumes. On the other hand, we calculate the electric field strengths $\boldsymbol{E}_0$ during the electric pulse ($\boldsymbol{U}_0$ = 1 V), and $\boldsymbol{E}_i$ at the beginning of the FVR ($\boldsymbol{U}_i \cong$ 12 mV), between the electrodes:

For the outer and inner electrode distances ($\boldsymbol{d}_o$ = 5 and $\boldsymbol{d}_i$ = 2.5 mm, respectively), the ratio of the respective fields is:

$$\frac{\bar{E}_i}{\bar{E}_0} = \frac{U_i/d_i}{U_0/d_0} = \frac{0.012\ V/0.0025\ m}{1\ V/0.005\ m} = \frac{4.8\ V/m}{200\ V/m} = 0.024 \tag{5}$$

This means, that free charges produced by the 1 V pulse during its 25 ms duration, were fixed in $\boldsymbol{k}_v = 0.024 = 2.4\%$ of the volume. Since only the liposomes can retain charges which sustain an electric potential in the subsequent acquisition time window, and thereby generate a FVR, almost the entire liposomal volume (= 2.5% from the sample volume, see Table II) should be polarized after expiration of the electric pulse.

If the observed magnetic field effect would be based on conformational changes on the liposome membrane surface, it should be accompanied by additional changes of the electric dipole moment, when effecting the DNLDS signal. The electric and magnetic forces F_E and F_M can be written as:

$$\bar{F}_E = \bar{E} \cdot Q \tag{6}$$

$$\bar{F}_M = \bar{H} \cdot \phi \tag{7}$$

where is Q the charge moved by the electric field E, and ϕ the magnetic flux (dimension V·m) at the magnetic field strength H (dimension A/m). They can be expressed by the (correctly named) magnetic flux density B (dimension Vs/m^2), the magnetic field constant in the vacuum $\mu_0 = 1.256 \cdot 10^{-6}$ Vs/Am, and a proper effective area A. This effective area may be assumed as bordered by two opposite inner electrodes (d = 2.5 mm, l = 2 mm) and encloses a cylindrical volume V, the "inner electrode space". The potential distribution between and outside the electrodes will show a contribution of < 1% of the signal outside these

Table II. Calculated physical properties of the EY liposome probes.

Liposome volume	V_l	$2.4 \cdot 10^{-21}$	m^3
Membrane volume per liposome	V_w	$4.83 \cdot 10^{-22}$	m^3/liposome
Liposome surface	A_l	$8.66 \cdot 10^{-24}$	m^2
Liposomes pro volume	n_l	$1.04 \cdot 10^{19}$	l/m^3
Average liposome distance	d_l	$4.59 \cdot 10^{-7}$	m
Liposomal fractional volume	k_v	2.48	%

borders. The totally shifted charge Q by B can be written by combining (6) and (7):

$$Q = \frac{\bar{B}^2 \cdot \bar{A}}{\bar{E} \cdot \mu_0} \tag{8}$$

Taking the liposome data shown in Table II, a charge dipole length d_e can be calculated for discrete electrons on the liposome surface, which match conditions of the electric field strength E and the magnetic field strength (better: flux density) B in the probe:

$$\bar{d}_e = \sqrt{\frac{Q \cdot \bar{A}_l}{n_l \cdot e}} \tag{9}$$

where is A_l the surface area of one liposome, n_l the number of liposomes inside the volume V, and e the elementary charge. Q will be inserted from (8).

In order to check the assumption of spin polarizations of membrane surface charges as a possible origin of sensitivity to weak magnetic fields, we calculate an electron coherence length λ by the *De Broglie* equation for an electron with the elementary charge e and mass m_e:

$$\lambda = \frac{h}{\sqrt{e \cdot U \cdot 2m_e}} \tag{10}$$

where h is the *Planck* number ($6.625 \cdot 10^{-34}$ Js), $e \cdot U$ presents an energy term, for which we will insert the kinetic one-electron energy level corresponding to the 1st harmonic of the DNLDS signal, similar as we have done for the dipole calculations upward, yielding λ = 11.2 nm.

Calculating a matching magnetic flux density B using equations 8 and 9, which leads to the condition $\lambda = d_e$, results in $B \sim 37$ G. This corresponds rather well to the local minimum of the 1. harmonic signal for EY liposome experiments (see Fig. 5).

In conclusion spin polarization processes of coupled surface charges on biological membranes could be a possible origin for the observed sensitivity to weak magnetic fields, or at least, could have a supplemental effect on other current discussed biological magnetic field reception mechanisms, like ICR or singlet-triplet mixing of radical pairs. Further investigations will be needed to relate this effect to biological receptor mechanisms for weak magnetic fields and ELF radiation.

Acknowledgement

The author thanks H. Scheer (München) for scientific care and frequent discussions for many years.

Adair R. K. (1997), Hypothetical biophysical mechanisms for the action of weak low frequency electromagnetic fields at the cellular level. Radiat. Prot. Dosim. **72**, 271–278.

Bultmann T., Lin H. N., Wang Z. Q., and Huang C. H. (1991), Thermotropic and mixing behavior of mixed-chain phosphatidylcholines with molecular weights identical with that of L-alpha-dipalmitoylphosphatidylcholine. Biochemistry **30**, 7194–202.

Chakkalakal D. A., Mollner T. J., Bogard M. R., Fritz E. D., Novak J. R., and McGuire M. H. (1999), Magnetic field induced inhibition of human osteosarcoma cells treated with adriamycin. Cancer Biochem. Biophys. **17**, 89–98.

Christopher J., Gregoriadis K., and Gregoriadis G. (1984), A simple procedure for preparing liposomes capable of high encapsulation efficiency under mild conditions. In: Liposome Technology (Gregory Gregoriadis, ed.), Vol. **1**. CRC-Press Boca Raton FL 1984, 19–26.

Collins D. S. (1995), Liposome preparation and material encapsulation method. Amgen Inc., Pat. No. 9512387, USA. Int. Appl. **94**, 34 pp.

Crasson M., Legros J. J., Scarpa P., and Legros W. (1999), 50 Hz Magnetic field exposure influence on human performance and psychophysiological parameters: two double-blind experimental studies. Bioelectromagnetics **20**, 474–486.

Darendeliler M. A., Darendeliler A., and Sinclair P. M. (1997), Effects of static magnetic and pulsed electromagnetic fields on bone healing. Int. J. Adult Orthodon. Orthognath. Surg. **12**, 43–53.

Davies E., Woodward A., and Kell D. (2000), The use of nonlinear dielectric spectroscopy to monitor the bioelectromagnetic effects of a weak pulsed magnetic field in real time. Bioelectromagnetics **21**, 25–33.

Deutschlander M. E., Phillips J. B., and Borland S. C. (1999), The case for light-dependent magnetic orientation in animals. J. Exp. Biol. **202**, 891–908.

Giudice E. Del, Fleischmann M., Preparata G., and Talpo G. (2002), On the "Unreasonable" Effects of ELF Magnetic Fields Upon a system of ions. Bioelectromagnetics **23**, 522–530.

Khizhenkov P. K., Dobritsa N. V., Netsvetov M. V., and Driban V. M. (2001), Influence of low- and superlow-frequency alternating magnetic fields on ionic permeability of cell membranes. Dopov. Nats. Akad. Nauk Ukr. **4**, 161–164.

Levchuk Y. N., and Volovik Z. N. (1983), Dimensions of lecithin liposomes formed by ultrasonication. Biofizika **28**, 266–9.

Liboff A. R. (1997), Electric field ion cyclotron resonance. Bioelectromagnetics **18**, 85–87.

Matsuzaki K., Murase O., Sugishita K., Yoneyama S., Akada K., Ueha M., Nakamura A., and Kobayashi S. (2000), Optical characterization of liposomes by right angle light scattering and turbidity measurement. Biochim. Biophys. Acta **1467**, 219–26.

McShea A., Woodward A. M., and Kell D. B. (1992), Nonlinear dielectric properties of *Rhodobacter capsulatus*. Bioelectrochem. Bioenerg. **29**, 205–14.

Ogrodnik A., Krueger H. W., Orthuber H., Haberkorn R., Michel-Beyerle M. E., and Scheer H. (1982), Recombination dynamics in bacterial photosynthetic reaction centers. Biophys. J. **39**, 91–9. 82.

Pazur A. (2001), Electric relaxation processes in lipid-bilayers after exposure to weak magnetic pulses. Z. Naturforsch. **56c**, 831–837.

Rademaker H., Hoff A. J., Van Grondelle R., and Duysens L. N. M. (1980), Carotenoid triplet yields in normal and deuterated *Rhodospirillum rubrum*. Biochim. Biophys. Acta **592**, 240–57.

Ramundo-Orlando A., Mattia F., Palombo A., and D'Inzeo G. (2000a), Effect of low frequency, low amplitude magnetic fields on the permeability of cationic liposomes entrapping carbonic anhydrase: II. No evidence for surface enzyme involvement. Bioelectromagnetics **21**, 499–507.

Ramundo-Orlando A., Morbiducci U., Mossa G., and D'Inzeo G. (2000b), Effect of low frequency, low amplitude magnetic fields on the permeability of cationic liposomes entrapping carbonic anhydrase: I. Evidence for charged lipid involvement. Bioelectromagnetics **21**, 491–498.

Santini M. T., Cametti C., Paradisi S., Straface E., Donelli G., Indovina P. L., and Malorni W. (1995), A 50 Hz sinusoidal magnetic field induces changes in the membrane electrical properties of K562 leukaemic cells. Bioelectrochem. Bioenerg. **36**, 39–45.

Smith S. D., McLeod B. R., and Liboff A. R. (1995), Testing the ion cyclotron resonance theory of electromagnetic field interaction with odd and even harmonic tuning for cations. Bioelectrochem. Bioenerg. **38**, 161–167.

Torres de Araujo F. F., Pires M. A., Frankel R. B., and Bicudo C. E. M. (1986), Magnetite and magnetotaxis in algae. Biophys. J. **50**, 375–378.

Waliszewski P., Skwarek R., Jeromin L., and Manikowski H. (1999), On the mitochondrial aspect of reactive oxygen species action in external magnetic fields. Photochem. Photobiol. **52**, 137–140.

Wiltschko R., Wiltschko W., and Munro U. (2000), Light-dependent magnetoreception in birds: the effect of intensity of 565-nm green light, Naturwissenschaften **87**, 366–369.

Woodward A. M., Jones A., Zhang X., Rowland J., and Kell D. B. (1996), Rapid and non-invasive quantification of metabolic substrates in biological cell suspensions using non-linear dielectric spectroscopy with multivariate calibration and artificial neural networks. Principles and applications. Bioelectrochem. Bioenerg. **40**, 99–132.

Woodward, A. M., Davies, E. A., Denyer S., Olliff C., and Kell D. B. (2000), Non-linear dielectric spectroscopy: antifouling and stabilization of electrodes by a polymer coating. Bioelectrochemistry **51**, 13–20.

Yardley J. E., Todd R., Nicholson D. J., Barrett J., Kell D. B., and Davey C. L. (2000), Correction of the influence of baseline artefacts and electrode polarization on dielectric spectra. Bioelectrochemistry **51**, 53–65.

Yee K., Lee C., Klingler, J. F., and McConnell H. M. (1994), Electric field-induced concentration gradients in lipid monolayers. Science **263**, 655–8.

Zhadin M. N., Novikov V. V., Barnes F. S., and Pergola N. F. (1998), Combined action of static and alternating magnetic fields on ionic current in aqueous glutamic acid solution. Bioelectromagnetics **19**, 41–45.

Zhadin M. N. (2001), Review of Russian literature on biological action of DC and low-frequency AC magnetic fields. Bioelectromagnetics **22**, 27–45.